THE AMERICAN SOCIETY OF MECHANICAL ENGINEERS
345 E. 47 St., New York, N.Y. 10017

85-APM-3

Please return to J. C. Trinkle

March 1985 52(1): 179-184

Clearing Maximum Height With Constrained Kinetic Energy

M. Hubbard
Department of Mechanical Engineering,
University of California,
Davis, Calif. 95616
Mem. ASME

J. C. Trinkle
Department of Systems Engineering,
University of Pennsylvania,
Philadelphia, Pa. 19104

This paper addresses the question: In order to clear a given height, defined as that which is passed over by all points in the moving body, what is the minimum initial kinetic energy required and what are the other conditions that specify the solution completely? An expression is derived for the height cleared above an original supporting ground plane. This transcendental expression is maximized numerically subject to certain equality and inequality constraints using nonlinear constrained optimization techniques. The optimal solution includes the height cleared and the required control variables. The parameter space of body descriptors in which the optimal solution is presented decomposes into two regions in which the solutions differ qualitatively.

Introduction

It is occasionally of interest to jump or to throw an object as high as possible with the height being defined as that which is cleared by all moving points in the object. This fundamental act forms the basis for many games, including several track and field events, has been practiced by almost all of us at one time or another in our lives, has some industrial applications, and has even inspired nursery rhymes. Yet, except for the particle ballistics problem so familiar to elementary physics students, there seems to have been little analytical study of the more general problem that includes the effects of the extended nature and geometrical shape of the moving body.

Conservation of energy in the case of a particle, of course, requires that the height cleared be a monotonic increasing function of initial kinetic energy. Intuitively, this carries over to the case of an extended (three-dimensional) rigid body and provides a conceptual framework for the problem formulation. One would also expect the height cleared by any connected set of rigid bodies to be a monotonic function of initial kinetic energy as long as the connections exhibit no dissipation or potential energy storage. With a given initial kinetic energy, what is the maximum height, which is possible for a body to clear (or equivalently, in order to clear a given height, what is the minimum initial kinetic energy required) and what are the other conditions that specify the solution completely?

In this paper a simple model for the extent of the body is assumed, but it is believed that similar techniques could be used for the solution with more complicated body shapes. An expression is derived for the height cleared, above an original supporting ground plane, in terms of the parameters that describe the body and its initial conditions. The maximization of this transcendental expression, subject to certain equality and inequality constraints on the variables, which arise naturally in the problem formulation, is necessarily accomplished numerically using nonlinear constrained optimization techniques. The parameter space of body descriptors in which the optimal solution (height cleared and the associated control variables that permit this) is presented, is shown to decompose into two regions in which the optimal solutions differ qualitatively.

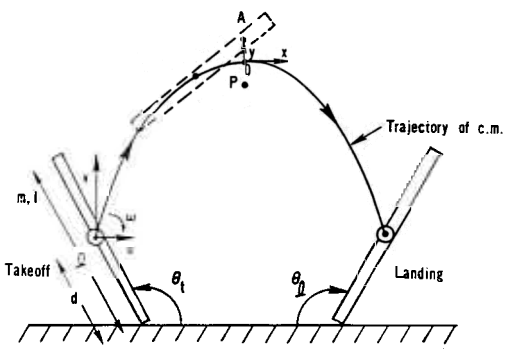

Fig. 1 Schematic diagram of model showing rod geometry, hypothetical center-of-mass trajectory, point *P* with maximum height cleared by all points in the rod, point *A* in rod above *P*, and point 0 at zenith of c.m. trajectory, the origin of *xy* frame

Model

Figure 1 shows a schematic diagram of the proposed motion. We consider the simplest possible model for the moving body, a thin rigid rod of length l, position of the center of mass along the rod d, mass m, and centroidal moment of inertia I. Further, the rod is assumed to move only

Contributed by the Applied Mechanics Division for presentation at the 1985 Joint ASME/ASCE Applied Mechanics, Fluids Engineering, and Bioengineering Conference, Albuquerque, N. Mex., June 24-26, 1985 of THE AMERICAN SOCIETY OF MECHANICAL ENGINEERS.

Discussion on this paper should be addressed to the Editorial Department, ASME, United Engineering Center, 345 East 47th Street, New York, N.Y. 10017, and will be accepted until two months after final publication of the paper itself in the JOURNAL OF APPLIED MECHANICS. Manuscript received by ASME Applied Mechanics Division, January, 1984; final revision, May 1984 Paper No. 85-APM-3.

Copies will be available until February, 1986.

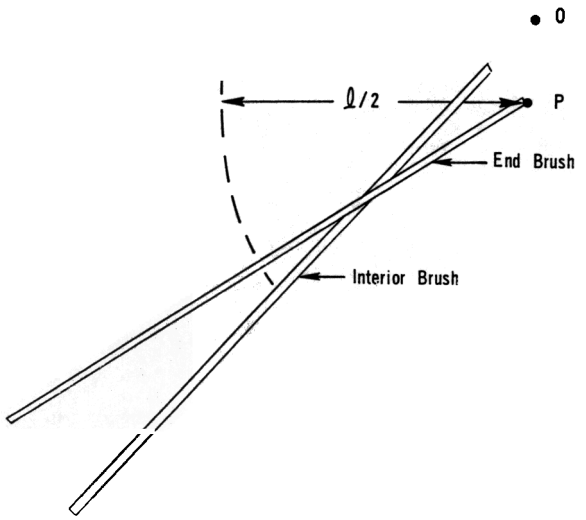

Fig. 2 Schematic of two possible rod positions at the first possible brush time, $-t_l$

under the influence of gravity in a vertical plane from an initial position which has at least one point of the rod in contact with the horizontal ground plane. Denote by P the fixed point (as yet unknown) with greatest height cleared by all points of the rod. This would be the position of the crossbar in an optimal high jump. Although the case with $d \neq l/2$ can be studied [1], in what follows we pick the simplest geometry, $d = l/2$.

Define an xy coordinate system with origin at 0, the (also unknown) zenith of the parabolic trajectory of the rod center of mass (c.m.) as shown in Fig. 1, and let $t = 0$ when the c.m. is at 0. Note that 0 must be either coincident with or above point P.

The final assumption concerns the symmetry of the optimal trajectory; the rod is taken to be horizontal when its center lies directly above P. This assumption is motivated from physical intuition and, based on a preliminary numerical study not reported here, is felt to be valid except possibly for extremely small initial kinetic energies. In this preliminary study the value of θ at $t = 0$ was allowed to vary freely together with the remaining variables to be discussed in the following and was always found to be zero.

Because of the choice of $t = 0$ when the c.m. is at $x = y = 0$, we may write particularly simple expressions for the velocities and positions of the c.m.

$$v_x = u = \text{constant} \qquad v_y = -gt \tag{1}$$

$$x = ut \qquad y = -\frac{gt^2}{2} \tag{2}$$

and the rod orientation

$$\theta = \omega t. \tag{3}$$

An Expression for the Height Cleared

From the definition of P, it is clear that the rod must touch (brush) P from above at least once during the motion (or else P would be able to be moved up, a contradiction). Consider now the point A on the rod (or rod extended) which lies directly above P and which varies throughout the rod during the motion. From kinematic considerations, we can write the vertical velocity of A as

$$\dot{h}_A = -gt + u \tan \omega t + u\omega t \sec^2 \omega t \tag{4}$$

the first term being the velocity of the rod c.m., the second the vertical component of the velocity of A relative to the c.m.,

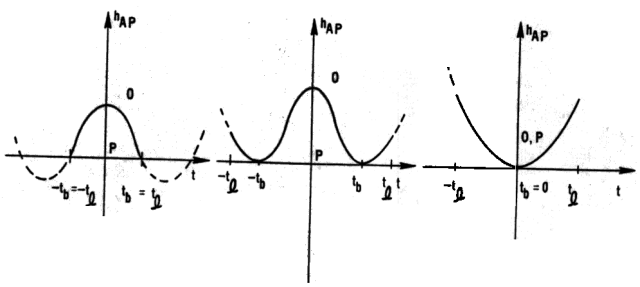

Fig. 3 h_{AP} versus t for (a) end brush ($t_b = t_l$), (b) noncentral interior brush ($2\tilde{\omega}\tilde{u} < 1$ and $t_b \neq 0$), and (c) central brush ($2\tilde{\omega}\tilde{u} \geq 1$ and $t_b = 0$)

and the last a term due to "convection." Integration of (4) gives an expression for the height h_{AP} of point A above P,

$$h_{AP}(t) = ut \tan \omega t - gt^2/2 + C. \tag{5}$$

Having chosen $t = 0$ when the rod c.m. is above P we denote by t_b the time of brush. We note that t_b may or may not be zero. When $t_b \neq 0$, then, by symmetry, brushes occur at both t_b and $-t_b$, but when $t_b = 0$ there is only one brush. Because of the symmetry assumed, various times introduced in the following enjoy a symmetry similar to that just described for t_b. For example, the take-off time t_l, while actually negative, has the same magnitude as the time of landing. To minimize unneccessary confusion resulting from signs of these quantities, the times (t_b, t_l, etc.) are taken in what follows to be positive whenever possible.

Because $h_{AP}(t_b) = 0$, the constant C in (5) may then be evaluated with the result that the geometric height loss (i.e., the height of the rod c.m. above point P at its zenith) is given by

$$h_{AP}(0) = h_{0P} = \epsilon = C = gt_b^2/2 - ut_b \tan \omega t_b. \tag{6}$$

The label "geometric height loss" is somewhat of a misnomer since, by definition, P is as high as possible. Yet it focuses the idea that, as is shown in what follows, it is generally optimal for A and P not to coincide ($\epsilon \neq 0$). In addition, the label distinguishes between "geometric height loss" and the height that is lost because kinetic energy is associated with rotation and horizontal translation rather than only with vertical translation.

Now the height of point 0 is known from energy conservation and take-off conditions; at take-off $t = t_l$, $v_y = v$ so that

$$h_0 = \frac{l}{2} \sin \omega t_l + v^2/2g. \tag{7}$$

Further, the initial kinetic energy is divided into three parts

$$T = mu^2/2 + mv^2/2 + I\omega^2/2 \tag{8}$$

which provides an expression for the elimination of v in what follows.

Now the object must be to maximize the height h_P which, using (6), (7), and (8), is given by

$$\begin{aligned} h_P &= h_0 - \epsilon \\ &= \frac{l}{2} \sin \omega t_l + T/mg - u^2/2g \\ &\qquad - I\omega^2/2mg - [gt_b^2/2 - ut_b \tan \omega t_b]. \end{aligned} \tag{9}$$

Defining dimensionless variables (denoted by $\sim$) $\tilde{T} = T/mgl$, $\tilde{I} = I/ml^2$, $\tilde{\epsilon} = \epsilon/l$, $\tilde{u} = u/\sqrt{lg}$, $\tilde{v} = v/\sqrt{lg}$, $\tilde{\omega} = \omega\sqrt{l/g}$, $\tilde{t}_l = t_l\sqrt{g/l}$, and $\tilde{t}_b = t_b\sqrt{g/l}$, we notice that (1) evaluated at t_l implies that $\tilde{v} = \tilde{t}_l$. The dimensionless height cleared $\tilde{h}_P = h_P/l$ can then be written as

$$\tilde{h}_P = \tilde{T} + (\sin \tilde{\omega}\tilde{t}_l - \tilde{u}^2 - \tilde{I}\tilde{\omega}^2 - \tilde{t}_b^2)/2 + \tilde{u}\tilde{t}_b \tan \tilde{\omega}\tilde{t}_b. \tag{10}$$

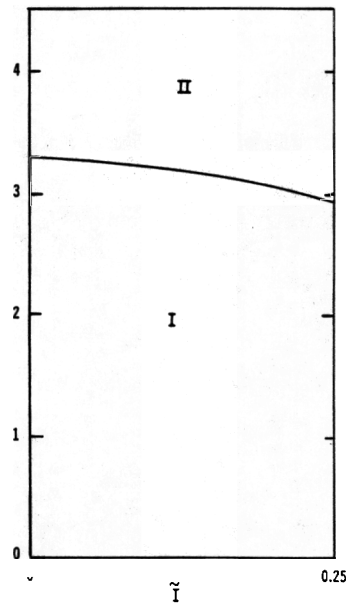

Fig. 4 $\tilde{T}, \tilde{I}$ solution space decomposes into two regions where interior brushes (*I*) and end brushes (*II*) are optimal, respectively

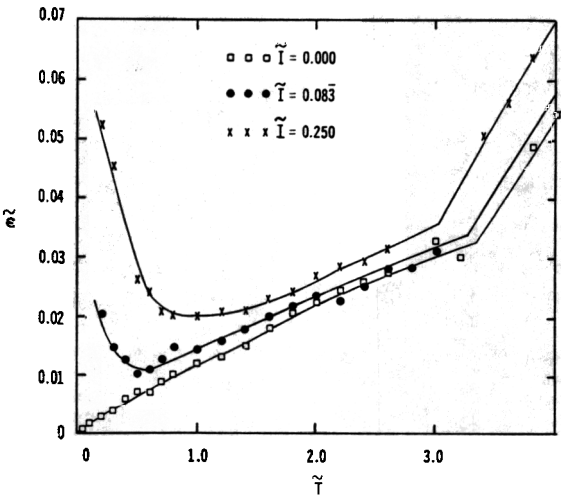

Fig. 5 Optimal $\tilde{\epsilon}$ versus $\tilde{T}$ with $\tilde{I}$ as parameter

In (10), the four independent variables $\tilde{\omega}$, $\tilde{u}$, $\tilde{t}_b$, and $\tilde{t}_l$ are to be chosen to maximize $\tilde{h}_P$, for given values of the parameters $\tilde{T}$, $\tilde{I}$ and subject to certain constraints. One of these constraints is the dimensionless form of (8) with v eliminated using (1),

$$2\tilde{T} = \tilde{I}\tilde{\omega}^2 + \tilde{u}^2 + \tilde{t}_l^2. \tag{11}$$

The remaining constraints on the independent variables arise from considerations that insure that a particular optimal solution $\tilde{\omega}$, $\tilde{u}$, $\tilde{t}_b$, $\tilde{t}_l$ results in a physically meaningful trajectory which passes *over* point P. The first of these is concerned with the fact that the brush time t_b in (6) is not completely arbitrary. We require that brush must occur at or after take-off (because this model treats only the airborne portion of the motion), which implies that the brush time must satisfy the inequality constraint

$$\tilde{t}_b \le \tilde{t}_l \tag{12}$$

Next we realize that brush can occur only at a time when the c.m. is on or within a circle of radius $l/2$ about point P. Defining the last (for $t_b > 0$) possible brush time, t_l, to be that time when the c.m. is on the above circle, we have from geometry that

$$(y(t_l) + \epsilon)^2 + x^2 = l^2/4. \tag{13}$$

The two cases of a first possible brush and an interior brush, defined in what follows, are schematically illustrated in Fig. 2.

Using relations (2) and (6) to eliminate y and x, and nondimensionalizing (13) gives

$$(\tilde{t}_l^2/2 - \tilde{\epsilon})^2 + (\tilde{u}\tilde{t}_l)^2 - 1/4 = 0 \tag{14}$$

a quadratic in $\tilde{t}_l^2$. Thus, the dimensionless last possible brush time is given by

$$\tilde{t}_l = \left[2(\tilde{\epsilon} - \tilde{u}^2) + \sqrt{4\tilde{u}^4 - 8\tilde{u}^2\tilde{\epsilon} + 1}\right]^{1/2} \tag{15}$$

where

$$\tilde{\epsilon} = \tilde{t}_b^2/2 - \tilde{u}\tilde{t}_b \tan \tilde{\omega}\tilde{t}_b. \tag{16}$$

Therefore, the second inequality constraint that the actual brush time must satisfy is

$$\tilde{t}_b \le \tilde{t}_l \tag{17}$$

where $\tilde{t}_l$ is related to the independent variables $\tilde{u}$, $\tilde{\omega}$, and $\tilde{t}_b$ by (15) and (16).

Whether or not constraint (17) is active turns out to be one of the most interesting features of the solution. In fact, the existence of a fourth constraint depends on the activity of (17). Obviously, $t_b < t_l$ corresponds to a brush in the interior of the rod, hereafter called an interior brush, while when $t_b = t_l$, brush occurs at the end of the rod. The position of the rod in these two cases, at time $-t_l$, is shown in Fig. 2. In the former case, point A approaches P from above, brushes P, and then departs from P from above, as illustrated schematically in Fig. 3(*b*). Here, clearly, $\dot{h}_{AP}(t_b) = 0$. However, in an end brush on the way up, it is possible for point A (on the rod extended) to be below P until the first possible brush time $-t_l$, after which point A is above P. This implies that $\dot{h}_{AP}(t_b) \ge 0$ when $t_b < 0$. This is illustrated in Fig. 3(*a*). When the positive brush time is considered, i.e., the brush on the way down, $t_b > 0$ and $\dot{h}_{AP}(t_b) \le 0$. The preceding possibilities can be expressed in terms of dimensionless quantities as

$$\text{if} \quad \tilde{t}_l - \tilde{t}_b > 0 \quad \text{then} \quad \dot{\tilde{h}}_{AP}(\tilde{t}_b) = -\tilde{t}_b + \tilde{u}\tan\tilde{\omega}\tilde{t}_b + \tilde{u}\tilde{\omega}\tilde{t}_b \sec^2\tilde{\omega}\tilde{t}_b = 0, \tag{18a}$$

$$\text{or else} \quad \tilde{t}_l - \tilde{t}_b = 0 \quad \text{and} \quad -\tilde{t}_b + \tilde{u}\tan\tilde{\omega}\tilde{t}_b + \tilde{u}\tilde{\omega}\tilde{t}_b \sec^2\tilde{\omega}\tilde{t}_b \le 0 \tag{18b}$$

$$\text{for} \quad \tilde{t}_l > 0, \quad \tilde{t}_b > 0.$$

Interior brushes can be further decomposed into two subclasses: central and noncentral. Consider (18*a*), the dimensionless form of (4). Obviously, the tangent term eventually dominates making $\dot{\tilde{h}}_{AP}$ large and positive. Also, for all parameter combinations, $\tilde{h}_{AP}(0) = 0$. For some parameter combinations, however, (when $\tilde{\omega}\tilde{u} \ge 1/2$), $\tilde{t}_b = 0$ is the *only* zero of (18*a*) and the $\tilde{h}_{AP}$ versus $\tilde{t}$ curve has only one minimum (at $\tilde{t}_b = 0$), as shown in Fig. 3(*c*). Large $\tilde{\omega}$ and $\tilde{u}$ represent energy that cannot be channeled into $\tilde{v}$ and hence result in a lower peak height for the c.m. Thus, from these considerations, it is seen that values for the parameters $\tilde{\omega}$, $\tilde{u}$ for which the product $2\tilde{\omega}\tilde{u} > 1$ cannot be optimal. Indeed, in the numerical solutions discussed in what follows this was verified.

The optimization problem can now be summarized as follows: maximize $\tilde{h}_P$ ($\tilde{\omega}$, $\tilde{u}$, $\tilde{t}_b$, $\tilde{t}_l$) given by (10) for given $\tilde{T}$ and $\tilde{I}$ and subject to constraints (11), (12), and (17) augmented by (15), (16), and (18). Note that all constraints are in terms of the independent variables $\tilde{\omega}$, $\tilde{u}$, $\tilde{t}_b$, $\tilde{t}_l$ and restrict the possible

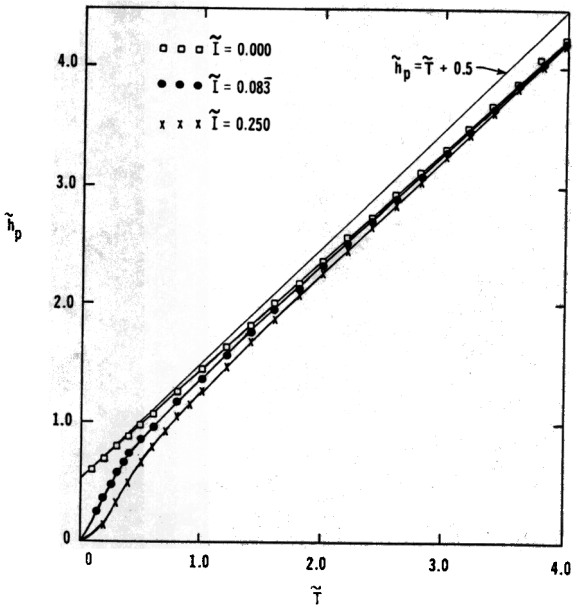

Fig. 6 Optimal $\tilde{h}_p$ versus $\tilde{T}$ with $\tilde{I}$ as parameter

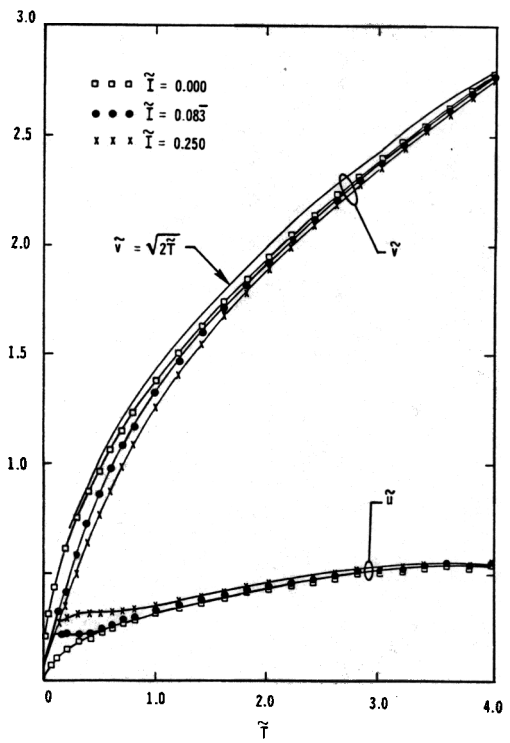

Fig. 7 Optimal $\tilde{v}$ and $\tilde{u}$ versus $\tilde{T}$ with $\tilde{I}$ as parameter

optimal solutions to a subset of the $\tilde{\omega}$, $\tilde{u}$, $\tilde{t}_b$, $\tilde{t}_t$ parameter four-space.

Numerical Solutions

Although the nonlinearity of the objective function (10) poses no problems, the rather complicated nature of the constraints motivates the use of numerical techniques to compute the solution. Over the last decade or two, dramatic advances have been made in the development of numerical methods and software for optimization [2, 3]. Even in the most complicated problem category, optimization with nonlinear inequality constraints (of which the present

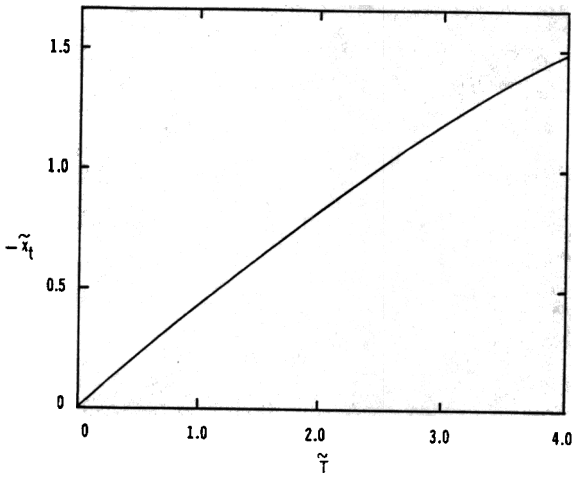

Fig. 8 Optimal $\tilde{x}_t$ versus $\tilde{T}$

problem is an example), such methods have become much more efficient and reliable, to the point where reasonable results are possible using routines from software libraries [4].

The numerical solutions presented in the following were calculated using a computer program written by one of us (J.T.) based on sequential augmented Lagrangian method [3]. Since the computations are necessarily exceedingly detailed, a check was made using an entirely different computer program using the canned subroutine E04VBF from the Numerical Algorithms Group software library NAGLIB [4]. This subroutine is also based on a sequential augmented Lagrangian method and utilizes analytic expressions for the derivatives of the objective function.

For a time it was felt that an additional constraint on the curvature of the geometric height lost,

$$\ddot{\tilde{h}}_{AP}(\tilde{t}_b) \geq 0,$$

might be needed to insure that the object passed over rather than under P. This was not found necessary, however, since when the initial guess for the solution was a feasible one (resulting in a trajectory that passed over P and for which

$$\ddot{\tilde{h}}_{AP}(\tilde{t}_b) > 0)$$

the search never passed the hyperplane

$$\ddot{\tilde{h}}_{AP}(\tilde{t}_b) = 0$$

and the eventual optimal solution always satisfied this most fundamental constraint.

The conditional nature of constraint (18) was handled in the following way. The entire problem was solved twice, once assuming constraint (17) to be inactive and once assuming (17) to be active. In the former case (case *I*), equality constraint (18*a*) was used. In the latter case (case *II*), inequality constraint (18*b*) was applied. The final solution was then taken to be the one that yielded the maximum objective function. Optimal solutions were generated on a grid in the $\tilde{T}$, $\tilde{I}$ space over the range $0.0 < \tilde{T} < 4.0$ at 0.2 intervals and for three values of $\tilde{I}$; 0, 0.0833 = 1/12 (a homogeneous thin rod), 0.25 (a double point mass dumbbell with half the mass at either end). Note that while $\tilde{T}$ is theoretically unlimited, $\tilde{I}$, is restricted by geometry to lie in the range $0 < \tilde{I} < 0.25$. In Figs. 5–9, results are shown parameterized for only these values of I, the two limiting cases, and a nominal intermediate value.

As shown in Fig. 4, one of the features of the solution is that the $\tilde{T}$, $\tilde{I}$ space decomposes into two regions (*I* and *II*) where brush occurs in the interior and on the end of the bar, respectively. Interestingly, on the $\tilde{T}$, $\tilde{I}$ grid that was investigated, a central brush with $\tilde{\epsilon} = 0$ was *never* found to be optimal, In region *II*, the c.m. can reach its peak significantly

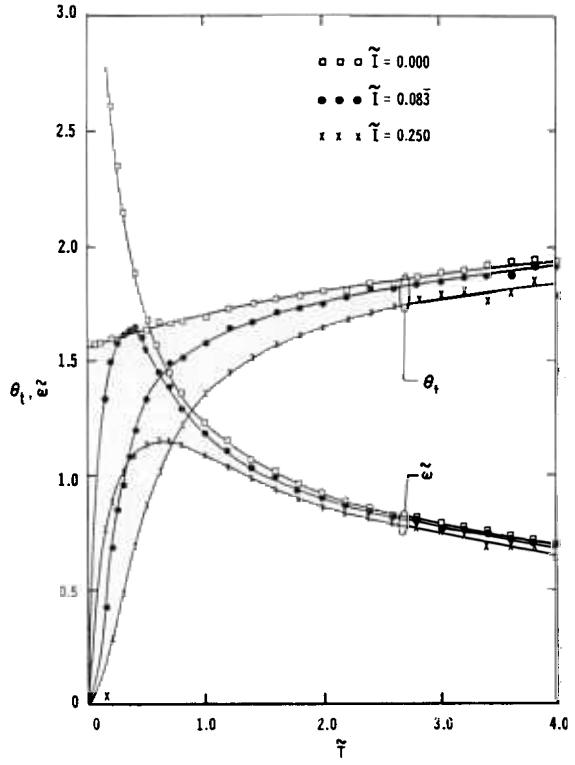

Fig. 9 Optimal θ_t and versus $\tilde{T}$ with $\tilde{I}$ as parameter

above the bar with relatively large geometric height loss, $\tilde{\epsilon} > 0.06$.

Figure 5 shows the geometric height loss $\tilde{\epsilon}$ versus $\tilde{T}$. The corners of the curves correspond to the boundary between regions *I* and *II* in Fig. 4. For a given energy $\tilde{T}$, the geometric height loss $\tilde{\epsilon}$ increases as $\tilde{I}$ increases, as would be expected since, for a given angular velocity, more energy must be stored in rotational motion. Yet an interesting fact is that even with $\tilde{I} = 0$, corresponding to a rod with negligible mass except at the c.m. and essentially no rotational energy storage, the optimal solution is still driven by geometric factors. It predicts nonzero horizontal velocity $\tilde{u}$ (see Fig. 7) and less cleared height than would be predicted from a pure energy balance. For nonzero $\tilde{I}$, there is an energy at which the geometric height loss is a minimum, with $\tilde{\epsilon}$ rising steeply for very small $\tilde{T}$ and more gradually for large $\tilde{T}$. The geometric height loss can be larger than $\tilde{\epsilon} = 0.05$ when $\tilde{I} = 0.25$ and $\tilde{T} < 0.2$ or $\tilde{T} > 3.0$.

Shown in Fig. 6 is the optimal objective function, $\tilde{h}_P$, the maximum height clearable with given energy $\tilde{T}$ and geometry $\tilde{I}$. As is apparent, the percent deviation from the upper bound, $\tilde{h}_P = \tilde{T} + 0.5$ representing the maximum achievable c.m. height, is largest for small energies $\tilde{T}$ and larger $\tilde{I}$. For $\tilde{T} = 0.4$ and $\tilde{I} = 0.25$, the maximum height clearable is less than 50 percent of the height achievable by the c.m. if clearance were not required. For large energies ($\tilde{T}>4.0$), the optimal height cleared becomes insensitive to $\tilde{I}$ and the three $\tilde{I}$ curves coalesce. This happens significantly below the $\tilde{h}_P = \tilde{T} + 0.5$ boundary, however, since both the geometric height loss and the horizontal and rotational kinetic energies required are substantial. Cusps similar to those in Fig. 5 are not apparent in Fig. 6, however.

The four important control parameters, $\tilde{v}$, $\tilde{u}$, θ_t, $\tilde{\omega}$ (governing take-off conditions completely) are shown in Figs. 7 and 9. Figure 7 plots vertical and horizontal take-off velocities $\tilde{v}$ and $\tilde{u}$ versus $\tilde{T}$ and shows that for given $\tilde{T}$, $\tilde{v}$ decreases as $\tilde{I}$ increases and more rotational energy is demanded. Also shown is an upper bounding curve

$$\tilde{v} = \sqrt{2\tilde{T}}$$

(analogous to the one in Fig. 6) corresponding to the case where all initial kinetic energy is associated with vertical motion. As noted previously, $\tilde{v} = -\tilde{t}_f$, so the $\tilde{v}$ curves in Fig. 7 can also be viewed as plots of half the time of flight. At low energies, the three $\tilde{v}$ curves for different $\tilde{I}$ are rather widespread, but they converge at higher energies, and thus the time of flight and maximum c.m. height become insenstive to moment of inertia variations at high energies. They also approach the boundary

$$\tilde{v} = \sqrt{2\tilde{T}}.$$

Thus, the percentage of kinetic energy wasted in rotation and horizontal translation gradually decreases as $\tilde{T}$ increases. In the low energy case, the smaller times of flight require larger angular velocities (see Fig. 9) for clearance and thus larger rotational kinetic energies, especially for large $\tilde{I}$.

Also shown in Fig. 7 is the horizontal velocity $\tilde{u}$. As $\tilde{T}$ increases $\tilde{u}$ also becomes increasingly less sensitive to both $\tilde{I}$ and $\tilde{T}$, but at a given $\tilde{T}$, $\tilde{u}$ *increases* with increasing $\tilde{I}$. This can be understood by remembering the role of $\tilde{u}$ in the expression (18*a*) for $\tilde{h}_{AP}$. As the product $\tilde{u}\tilde{\omega}$ approaches 0.5, the $\tilde{h}_{AP}$ profile becomes flatter and more like Fig. 3(*c*), thus decreasing $\tilde{\epsilon}$. Thus, there is an incentive for the product $\tilde{u}\tilde{\omega}$ to remain reasonably near 0.5.

Note that, since $\tilde{v} = \tilde{t}_f$, the dimensionless initial x position of the center of mass, the only remaining take-off parameter not yet discussed, can be computed from $\tilde{x}_i = -\tilde{u}\tilde{v}$. Figure 8 shows $\tilde{x}_i$ versus $\tilde{T}$. As is clear from the figure, $-\tilde{x}_i$ gradually gets larger with increasing $\tilde{T}$ but is quite insensitive to $\tilde{I}$. Indeed, it was impossible to discern, within the accuracy of our numerical solutions, any regular variation of $\tilde{x}_i$ with $\tilde{I}$. Thus, only one curve is plotted.

Figure 9 portrays the rotational aspects ($\tilde{\omega}$ and θ_t) of the optimal trajectories. For small $\tilde{T}$ and especially for large $\tilde{I}$, the small take-off angles θ_t imply that a rather severe compensation (a sacrifice in initial c.m. height) must be made to decrease the required rotational kinetic energy. For large energies, however, the take-off angle becomes insensitive to both $\tilde{T}$ and $\tilde{I}$, remaining in the region slightly greater than vertical ($\pi/2$).

For low energies $\tilde{T}<1.0$ and nonzero moments of inertia $\tilde{I}$, the angular velocity $\tilde{\omega}$ reaches a maximum value. Below this point there is simply not enough kinetic energy available to allow large $\tilde{\omega}$, while for larger energies $\tilde{T}$ more time is available to achieve a horizontal attitude at the zenith and hence large angular velocities (and large rotational kinetic energies) are not needed. Thus, as $\tilde{T}$ increases beyond 1.0, $\tilde{\omega}$ decreases continuously and becomes, as do all other variables, less sensitive to $\tilde{I}$.

Summary and Conclusions

For the first time, an expression has been derived for the height cleared by an object in terms of the parameters that describe the object and its initial conditions and which accounts for the fact that any point in the object may limit the height cleared. Numerical nonlinear optimization techniques were used to maximize this transcendental expression subject to both equality and inequality constraints arising naturally in the problem formulation. Although a simple extent model for the object was used, similar techniques could be used for the solution in the case of more complicated body shapes.

Important aspects of the optimal solution are the following:

1. For given initial energy, the maximum height cleared by an object is less for larger moments of inertia and in the case of low energies can be less than half of the maximum achievable c.m. height for the same energy.
2. The $\tilde{T}$, $\tilde{I}$ space decomposes into two regions where the

brush characteristics differ qualitatively. Roughly speaking, for energy-inertia combinations satisfying $\bar{T} + 1.5\ \bar{I} > 3.3$, it is optimal to brush the highest point with the end of the rod, while when $\bar{T} + 1.5\ \bar{I} < 3.3$, a brush in the interior of the rod is optimal.

3. It is always optimal for brush to occur at times other than when the c.m. is at its zenith 0. Thus the highest point P cleared always lies below 0. This geometric height loss is a complicated function of the initial energy and can be more than 7 percent of the rod length when $\bar{T} \geq 4$ and $\bar{I} = 0.25$.

A specific application of the general theory presented in this paper is to a rather simple model of Fosbury-flop high jumping [5] where the jumper moves more or less in a plane perpendicular to the crossbar. In this case, the energies $\bar{T}$ are usually considerably less than 1.0 and the moment of inertia $\bar{I}$ is probably near 0.083.

References

1 Hubbard, M., and Trinkle, J. C., "Optimal Initial Conditions for the Eastern Roll High Jump," in: *Biomechanics: Principles and Applications*, Huiskes, R., Van Campen, D. and DeWijn, J., eds., Martinus Nijhoff, The Hague, 1982, pp. 169–174.

2 Gill, P. E., and Murray, W., eds., *Numerical Methods for Unconstrained Optimization*, Academic Press, New York, 1974.

3 Gill, P. E., Murray, W., and Wright, M. H., *Practical Optimization*, Academic Press, New York, 1981.

4 NAG Fortran Library Reference Manual (Mark 8), Numerical Algorithms Group Limited, Oxford, England, 1981.

5 Hubbard, M., and Trinkle, J. C., "Optimal Fosbury-Flop High Jumping," *Proceedings of the Ninth International Congress of Biomechanics*, Waterloo, Ontario, Canada, Aug. 1983, in press.

Printed in U.S.A.